PHYSICAL REVIEW A VOLUME 45, NUMBER 2 15 JANUARY 1992

Stochastic Runge-Kutta algorithms. II. Colored noise

Rebecca L. Honeycutt
David Taylor Research Center, Code 1945, Bethesda, Maryland 20084-5000
(Received 6 June 1991)

Both a second-order and a fourth-order stochastic extension of standard Runge-Kutta algorithms are developed for colored-noise equations. These algorithms are tested by computing mean first-passage times in a bistable potential driven by colored noise.

PACS number(s): 05.40.+j, 02.50.+s, 02.60.+y

I. INTRODUCTION

In part I of this work (preceding paper), algorithms for integrating white-noise equations were developed. But for most systems white noise is not an accurate approximation to the actual fluctuations which occur. For such systems, colored-noise equations provide a more accurate description [1–3]. The defining equation becomes

$$\dot{x}=f(x)+\epsilon(t)\ , \tag{1.1}$$

where ϵ is the colored-noise variable. In this paper, we will use exponentially correlated, Gaussian colored noise with zero mean. The correlation properties of ϵ can be written as

$$\langle \epsilon(t)\rangle=0\ , \tag{1.2a}$$

$$\langle \epsilon(t)\epsilon(t')\rangle=D\lambda\exp(-\lambda|t-t'|)\ , \tag{1.2b}$$

where D is the noise strength and λ is the inverse of the correlation time, τ.

The one-dimensional colored-noise equation (1.1) with properties (1.2) can be replaced with the two-dimensional white-noise equations

$$\dot{x}=f(x,\epsilon)\ , \tag{1.3a}$$

$$\dot{\epsilon}=h(\epsilon)+\lambda g_w(t)\ , \tag{1.3b}$$

where $f(x,\epsilon)=f(x)+\epsilon$, $h(\epsilon)=-\lambda\epsilon$, and g_w is as defined in part I. The properties of ϵ are now

$$\{\langle \epsilon(t)\rangle\}=0\ , \tag{1.4a}$$

$$\{\langle \epsilon(t)\epsilon(t')\rangle\}=D\lambda\exp(-\lambda|t-t'|)\ , \tag{1.4b}$$

where $\langle\ \rangle$ indicates the white-noise average and $\{\ \}$ indicates averaging over the initial ϵ distribution

$$P(\epsilon_0)=(2\pi D\lambda)^{-1/2}\exp(-\epsilon_0^2/2D\lambda)\ . \tag{1.5}$$

II. EXPANSION OF ϵ AND x

The method of extending one-variable Runge-Kutta (RK) methods will now be broadened to include two-variable RK algorithms [4]. Using the same integration techniques as before, $\epsilon(\Delta t)$ expands to [5]

$$\epsilon(\Delta t)=\epsilon_0+h\sum_i h_\epsilon^{i-1}\frac{\Delta t^i}{i!}+\lambda\sum_i h_\epsilon^i\Gamma_i(\Delta t)\ , \tag{2.1}$$

where both summations are infinite: the first starting at $i=1$ and the second starting at $i=0$. Using the definition of Γ given in part I, and making the substitutions for h and h_ϵ, this expression can be written as

$$\epsilon(\Delta t)=\epsilon_0 e^{-\lambda\Delta t}+\int_0^{\Delta t}\lambda e^{-\lambda(\Delta t-\tau)}g_w(\tau)d\tau\ . \tag{2.2}$$

This is exactly the expression of $\epsilon(\Delta t)$ of the integral algorithm of Fox *et al.* [1]. Writing this expression without terms of Δt^5 or higher gives

$$\epsilon(\Delta t)=\epsilon_0+\Delta t h+\tfrac{1}{2}\Delta t^2 hh_\epsilon+\tfrac{1}{6}\Delta t^3 hh_\epsilon^2+\tfrac{1}{24}\Delta t^4 hh_\epsilon^3+R(\Delta t)\ , \tag{2.3a}$$

where

$$R(\Delta t)=\lambda\Gamma_0(\Delta t)+\lambda h_\epsilon\Gamma_1(\Delta t)+\lambda h_\epsilon^2\Gamma_2(\Delta t)+\lambda h_\epsilon^3\Gamma_3(\Delta t)+\lambda h_\epsilon^4\Gamma_4(\Delta t)\ . \tag{2.3b}$$

This can also be found from Eq. (2.5) of part I with the following substitutions:

$$x=\epsilon,\quad f=h,\quad f^{(1)}=h_\epsilon\ ,$$
$$f^{(i)}=0,\quad i=2,3,\ldots$$
$$\Gamma_i=\lambda\Gamma_i\ .$$

The mean and variance of $R(\Delta t)$ are found to be [5]

$$\langle R(\Delta t)\rangle=0 \tag{2.4a}$$

and

$$\langle R^2(\Delta t)\rangle=2D\lambda^2\Delta t(1+\Delta t h_\epsilon+\tfrac{2}{3}\Delta t^2 h_\epsilon^2+\tfrac{1}{3}\Delta t^3 h_\epsilon^3)\ . \tag{2.4b}$$

Applying the same expansion technique, but in two variables, $x(\Delta t)$ becomes

$$x(\Delta t)=x_0+\Delta t f+\tfrac{1}{2}\Delta t^2(f_\epsilon h+ff_x)+\tfrac{1}{6}\Delta t^3(f_\epsilon hh_\epsilon+f_xf_\epsilon h+f^2f_{xx}+ff_x^2)$$
$$+\tfrac{1}{24}\Delta t^4(f_\epsilon hh_\epsilon^2+f_xf_\epsilon hh_\epsilon+3ff_\epsilon f_{xx}h+4f^2f_xf_{xx}+f^3f_{xxx}+ff_x^3+f_x^2f_\epsilon h)+S(\Delta t) \tag{2.5a}$$

where

$$S(\Delta t)=\lambda\Gamma_1(\Delta t)f_\epsilon+\lambda\Gamma_2(\Delta t)(f_\epsilon h_\epsilon+f_xf_\epsilon)+\lambda\Gamma_3(\Delta t)(f_\epsilon h_\epsilon^2+f_xf_\epsilon h_\epsilon+f_x^2f_\epsilon)$$
$$+\tfrac{1}{2}f_{xx}f_\epsilon^2\int_0^{\Delta t}\lambda^2\Gamma_1^2(t')dt'+ff_\epsilon f_{xx}\int_0^{\Delta t}\lambda t'\Gamma_1(t')dt' . \tag{2.5b}$$

The mean and variance of $S(\Delta t)$ are found to be [5]

$$\langle S(\Delta t)\rangle=\tfrac{1}{24}\Delta t^4(2D\lambda^2)f_{xx}f_\epsilon^2 \tag{2.6a}$$

and

$$\langle S^2(\Delta t)\rangle=2D\lambda^2\Delta t[\tfrac{1}{3}\Delta t^2f_\epsilon^2+\tfrac{1}{4}\Delta t^3f_\epsilon(f_\epsilon h_\epsilon+f_xf_\epsilon)] . \tag{2.6b}$$

III. SECOND-ORDER EXTENSION

Following the same extension pattern as the one-dimensional case, the form used to extend the two-dimensional RK algorithm of second order (RKII) [4] is

$$x(\Delta t)=x_0+\tfrac{1}{2}\Delta t(F_1+F_2) , \tag{3.1a}$$

$$\epsilon(\Delta t)=\epsilon_0+\tfrac{1}{2}\Delta t(H_1+H_2)+(2D\lambda^2\Delta t)^{1/2}\phi_0 , \tag{3.1b}$$

where

$$H_1=h(\epsilon_0+(2D\lambda^2\Delta t)^{1/2}\phi_1) , \tag{3.2a}$$

$$H_2=h(\epsilon_0+\Delta tH_1+(2D\lambda^2\Delta t)^{1/2}\phi_2) , \tag{3.2b}$$

$$F_1=f(x_0,\epsilon_0+(2D\lambda^2\Delta t)^{1/2}\phi_1) , \tag{3.3a}$$

$$F_2=f(x_0+\Delta tF_1,\epsilon_0+\Delta tH_1+(2D\lambda^2\Delta t)^{1/2}\phi_2) . \tag{3.3b}$$

As with the one-variable case, the deterministic portions are the same as a typical two-dimensional RKII. Also ϕ_0, ϕ_1, and ϕ_2 are Gaussian random variables with zero mean and correlation properties that are yet to be determined. Since g_w only appears in the ϵ equation, no random terms have been attached to the $x(\Delta t)$ equation, or to the x argument of f. If a system were described with two equations, each driven by white noise, then random terms would appear in both equations of (3.1) and both arguments of f.

Expanding H_1, H_2, F_1, and F_2 yields

$$\epsilon(\Delta t)=\epsilon_0+\Delta th+\tfrac{1}{2}\Delta t^2hh_\epsilon+R'(\Delta t) , \tag{3.4a}$$

where

$$R'(\Delta t)=(2D\lambda^2\Delta t)^{1/2}[\phi_0+\tfrac{1}{2}\Delta t(\phi_1+\phi_2)h_\epsilon+\tfrac{1}{2}\Delta t^2\phi_1h_\epsilon^2] \tag{3.4b}$$

and

$$x(\Delta t)=x_0+\Delta tf+\tfrac{1}{2}\Delta t^2(ff_x+hf_\epsilon)+S'(\Delta t) , \tag{3.5a}$$

where

$$S'(\Delta t)+(2D\lambda^2\Delta t)^{1/2}[\tfrac{1}{2}\Delta tf_\epsilon(\phi_1+\phi_2)$$
$$+\tfrac{1}{2}\Delta t^2\phi_1(f_\epsilon h_\epsilon+f_\epsilon f_x)] . \tag{3.5b}$$

Comparing (3.4) and (3.5) with (2.3) and (2.5) shows the agreement of the deterministic portions. Since the ϕ's have mean zero, both $R'(\Delta t)$ and $S'(\Delta t)$ have mean zero in agreement with (2.4a) and (2.6a), respectively. The variances of the stochastic terms are

$$\langle R'^2(\Delta t)\rangle=2D\lambda^2\Delta t[\langle\phi_0^2\rangle+\Delta th_\epsilon\langle\phi_0(\phi_1+\phi_2)\rangle] \tag{3.6}$$

and

$$\langle S'^2(\Delta t)\rangle=0 . \tag{3.7}$$

Since $\langle S^2(\Delta t)\rangle$ and $\langle S'^2(\Delta t)\rangle$ are both of higher order than Δt^2, no additional information is obtained from (3.7). Equating the coefficients of $\langle R^2(\Delta t)\rangle$ and $\langle R'^2(\Delta t)\rangle$ results in

$$\langle\phi_0^2\rangle=1 \tag{3.8a}$$

and

$$\langle\phi_0(\phi_1+\phi_2)\rangle=1 . \tag{3.8b}$$

Equation (3.8b) implies that ϕ_1 and ϕ_0 are correlated and/or ϕ_2 and ϕ_0 are correlated. Since there are two equations and three unknowns the system is underdetermined. As with the white-noise case, we assume that $\phi_i=a_i\psi$, where ψ is a Gaussian random variable with mean zero and variance one. Of the possible solutions [5], we have chosen $a_0=1$, $a_1=0$, and $a_2=1$ to maintain consistency with the one-dimensional case. The resulting two-variable stochastic RKII is

$$x(\Delta t)=x_0+\tfrac{1}{2}\Delta t(F_1+F_2) , \tag{3.9a}$$

$$\epsilon(\Delta t)=\epsilon_0+\tfrac{1}{2}\Delta t(H_1+H_2)+(2D\lambda^2\Delta t)^{1/2}\psi , \tag{3.9b}$$

with

$$H_1=h(\epsilon_0) , \tag{3.10a}$$

$$H_2=h(\epsilon_0+\Delta tH_1+(2D\lambda^2\Delta t)^{1/2}\psi) , \tag{3.10b}$$

$$F_1=f(x_0,\epsilon_0) , \tag{3.11a}$$

$$F_2=f(x_0+\Delta tF_1,\epsilon_0+\Delta tH_1+(2D\lambda^2\Delta t)^{1/2}\psi) . \tag{3.11b}$$

IV. FOURTH-ORDER EXTENSION

Following the same procedure as the stochastic RKII (SRKII), the RK algorithm of fourth order (RKIV) [4] will be extended as

$$x(\Delta t)=x_0+\tfrac{1}{6}\Delta t(F_1+2F_2+2F_3+F_4)\ , \tag{4.1a}$$

$$\epsilon(\Delta t)=\epsilon_0+\tfrac{1}{6}\Delta t(H_1+2H_2+2H_3+H_4)+(D\lambda^2\Delta t)^{1/2}\phi_0\ , \tag{4.1b}$$

where

$$H_1=h(\epsilon_0+(D\lambda^2\Delta t)^{1/2}\phi_1)\ , \tag{4.2a}$$

$$H_2=h(\epsilon_0+\tfrac{1}{2}\Delta tH_1+(D\lambda^2\Delta t)^{1/2}\phi_2)\ , \tag{4.2b}$$

$$H_3=h(\epsilon_0+\tfrac{1}{2}\Delta tH_2+(D\lambda^2\Delta t)^{1/2}\phi_3)\ , \tag{4.2c}$$

$$H_4=h(\epsilon_0+\Delta tH_3+(D\lambda^2\Delta t)^{1/2}\phi_4) \tag{4.2d}$$

and

$$F_1=f(x_0,\epsilon_0+(D\lambda^2\Delta t)^{1/2}\phi_1)\ , \tag{4.3a}$$

$$F_2=f(x_0+\tfrac{1}{2}\Delta tF_1,\epsilon_0+\tfrac{1}{2}\Delta tH_1+(D\lambda^2\Delta t)^{1/2}\phi_2)\ , \tag{4.3b}$$

$$F_3=f(x_0+\tfrac{1}{2}\Delta tF_2,\epsilon_0+\tfrac{1}{2}\Delta tH_2+(D\lambda^2\Delta t)^{1/2}\phi_3)\ , \tag{4.3c}$$

$$F_4=f(x_0+\Delta tF_3,\epsilon_0+\Delta tH_3+(D\lambda^2\Delta t)^{1/2}\phi_4)\ . \tag{4.3d}$$

Again a standard deterministic portion has been used. Expanding the H_i's and F_i's leads to [5]

$$\epsilon(\Delta t)=\epsilon_0+\Delta th+\tfrac{1}{2}\Delta t^2hh_\epsilon+\tfrac{1}{6}\Delta t^3hh_\epsilon^2+\tfrac{1}{24}\Delta t^4hh_\epsilon^3+R'(\Delta t)\ , \tag{4.4a}$$

where

$$R'(\Delta t)=(D\lambda^2\Delta t)^{1/2}[\phi_0+\tfrac{1}{6}\Delta th_\epsilon(\phi_1+2\phi_2+2\phi_3+\phi_4)+\tfrac{1}{6}\Delta t^2h_\epsilon^2(\phi_1+\phi_2+\phi_3)+\tfrac{1}{12}\Delta t^3h_\epsilon^3(\phi_1+\phi_2)] \tag{4.4b}$$

and $x(\Delta t)$ to

$$x(\Delta t)=x_0+\Delta tf+\tfrac{1}{2}\Delta t^2(f_\epsilon h+ff_x)+\tfrac{1}{6}\Delta t^3[f^2f_{xx}+f_\epsilon hh_\epsilon+f_x(f_\epsilon h+ff_x)]+\tfrac{1}{24}\Delta t^4(f^3f_{xxx}+4f^2f_xf_{xx}+3ff_{xx}f_\epsilon h+f_\epsilon hh_\epsilon^2+f_xf_\epsilon hh_\epsilon+f_x^2f_\epsilon h+ff_x^3)+S'(\Delta t)\ , \tag{4.5a}$$

where

$$S'(\Delta t)=(D\lambda^2\Delta t)^{1/2}\{\tfrac{1}{6}\Delta tf_\epsilon(\phi_1+2\phi_2+2\phi_3+\phi_4)+\tfrac{1}{6}\Delta t^2(f_\epsilon h_\epsilon+f_\epsilon f_x)(\phi_1+\phi_2+\phi_3)+\tfrac{1}{12}\Delta t^3[f_\epsilon h_\epsilon^2+f_x(f_\epsilon h_\epsilon+f_\epsilon f_x)](\phi_1+\phi_2)\}+\tfrac{1}{12}\Delta t^3(D\lambda^2\Delta t)^{1/2}ff_{xx}f_\epsilon[(\phi_1+\phi_2+2\phi_3)(\phi_1+\phi_2)]+\tfrac{1}{24}\Delta t^3(D\lambda^2\Delta t)f_\epsilon^2f_{xx}[(\phi_1^2+\phi_2^2+2\phi_3^2)]\ . \tag{4.5b}$$

The resulting statistical properties are

$$\langle R'(\Delta t)\rangle=0\ , \tag{4.6a}$$

$$\langle R'^2(\Delta t)\rangle=D\lambda^2\Delta t[\langle\phi_0^2\rangle+\tfrac{1}{3}\Delta th_\epsilon\langle\phi_0(\phi_1+2\phi_2+2\phi_3+\phi_4)\rangle+\tfrac{1}{36}\Delta t^2h_\epsilon^2\langle(\phi_1+2\phi_2+2\phi_3+\phi_4)^2+12\phi_0(\phi_1+\phi_2+\phi_3)\rangle+\tfrac{1}{18}\Delta t^3h_\epsilon^3\langle(\phi_1+2\phi_2+2\phi_3+\phi_4)(\phi_1+\phi_2+\phi_3)+3\phi_0(\phi_1+\phi_2)\rangle]\ , \tag{4.6b}$$

$$\langle S'(\Delta t)=\tfrac{1}{24}\Delta t^4D\lambda^2f_\epsilon^2f_{xx}\langle\phi_1^2+\phi_2^2+2\phi_3^2\rangle\ , \tag{4.7a}$$

and

$$\langle S'^2(\Delta t)\rangle=D\lambda^2\Delta t[\tfrac{1}{36}\Delta t^2f_\epsilon^2\langle(\phi_1+2\phi_2+2\phi_3+\phi_4)^2\rangle+\tfrac{1}{18}\Delta t^3f_\epsilon^2(f_x+h_\epsilon)\langle(\phi_1+2\phi_2+2\phi_3+\phi_4)(\phi_1+\phi_2+\phi_3)\rangle]\ . \tag{4.7b}$$

Equating coefficients of (4.6) and (4.7) with the coefficients of (2.4) and (2.6) leads to seven equations which simplify to [5]

$$\begin{aligned}
&\langle \phi_0^2 \rangle = 2 , \\
&\langle \phi_0(\phi_2+\phi_4) \rangle = 3 , \\
&\langle \phi_0\phi_3 \rangle = 1 , \\
&\langle \phi_0(\phi_1+\phi_2) \rangle = 1 , \\
&\langle (\phi_1+2\phi_2+2\phi_3+\phi_4)^2 \rangle = 24 , \\
&\langle (\phi_1+2\phi_2+2\phi_3+\phi_4)(\phi_1+\phi_2+\phi_3) \rangle = 9 , \\
&\langle \phi_1^2+\phi_2^2+2\phi_3^2 \rangle = 2 .
\end{aligned} \tag{4.8}$$

Unlike the previous two cases, these seven independent equations overdetermine the system. Therefore if we are to obtain a solution, more than five variables will be needed. Define

$$\phi_i \equiv a_i\psi_1 + b_i\psi_2 , \tag{4.9}$$

where ψ_1 and ψ_2 are Gaussian random numbers with the properties $\langle \psi_i \rangle = 0$ and $\langle \psi_i\psi_j \rangle = \delta_{ij}$. We have chosen the following solution to the equations created from this definition:

$$\begin{aligned}
&a_0 = 1, \quad b_0 = 1 , \\
&a_1 = \tfrac{1}{4} + \frac{\sqrt{3}}{6}, \quad b_1 = \tfrac{1}{4} - \frac{\sqrt{3}}{6} + \frac{\sqrt{6}}{12} , \\
&a_2 = \tfrac{1}{4} + \frac{\sqrt{3}}{6}, \quad b_2 = \tfrac{1}{4} - \frac{\sqrt{3}}{6} - \frac{\sqrt{6}}{12} , \\
&a_3 = \tfrac{1}{2} + \frac{\sqrt{3}}{6}, \quad b_3 = \tfrac{1}{2} - \frac{\sqrt{3}}{6} , \\
&a_4 = \tfrac{5}{4} + \frac{\sqrt{3}}{6}, \quad b_4 = \tfrac{5}{4} - \frac{\sqrt{3}}{6} + \frac{\sqrt{6}}{12} .
\end{aligned}$$

The resulting SRKIV is

$$x(\Delta t) = x_0 + \tfrac{1}{6}\Delta t (F_1 + 2F_2 + 2F_3 + F_4) , \tag{4.10a}$$

$$\epsilon(\Delta t) = \epsilon_0 + \tfrac{1}{6}\Delta t (H_1 + 2H_2 + 2H_3 + H_4) + (D\lambda^2\Delta t)^{1/2}(\psi_1 + \psi_2) , \tag{4.10b}$$

with

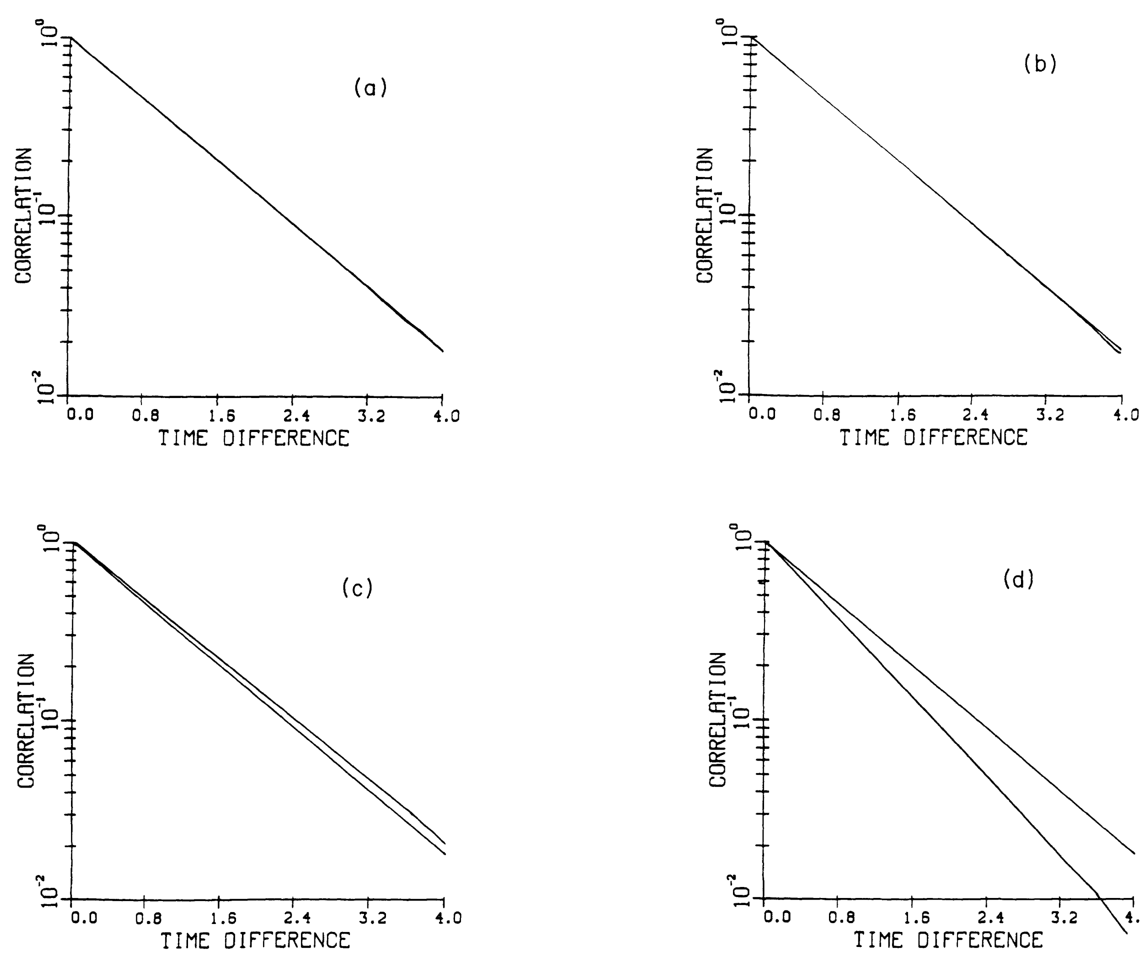

FIG. 1. The correlation of the simulated colored noise is compared to the theoretical correlation. For each of the plots, $\tau = 1.0$, $\Delta t = 0.4$, 100 initial ϵ values were used, and 10 000 time averages were taken. The straight line in each plot is the theoretical correlation. The other line is due to the (a) integral algorithm, (b) SRKIV algorithm, (c) SRKII algorithm, and (d) Euler algorithm.

$$H_1 = h(\epsilon_0 + (D\lambda^2\Delta t)^{1/2}(a_1\psi_1 + b_1\psi_2)) , \quad (4.11a)$$

$$H_2 = h(\epsilon_0 + \tfrac{1}{2}\Delta t H_1 + (D\lambda^2\Delta t)^{1/2}(a_2\psi_1 + b_2\psi_2)) , \quad (4.11b)$$

$$H_3 = h(\epsilon_0 + \tfrac{1}{2}\Delta t H_2 + (D\lambda^2\Delta t)^{1/2}(a_3\psi_1 + b_3\psi_2)) , \quad (4.11c)$$

$$H_4 = h(\epsilon_0 + \Delta t H_3 + (D\lambda^2\Delta t)^{1/2}(a_4\psi_1 + b_4\psi_2)) \quad (4.11d)$$

and

$$F_1 = f(x_0, \epsilon_0 + (D\lambda^2\Delta t)^{1/2}(a_1\psi_1 + b_1\psi_2)) , \quad (4.12a)$$

$$F_2 = f(x_0 + \tfrac{1}{2}\Delta t F_1, \epsilon_0 + \tfrac{1}{2}\Delta t H_1 + (D\lambda^2\Delta t)^{1/2}(a_2\psi_1 + b_2\psi_2)) , \quad (4.12b)$$

$$F_3 = f(x_0 + \tfrac{1}{2}\Delta t F_2, \epsilon_0 + \tfrac{1}{2}\Delta t H_2 + (D\lambda^2\Delta t)^{1/2}(a_3\psi_1 + b_3\psi_2)) , \quad (4.12c)$$

$$F_4 = f(x_0 + \Delta t F_3, \epsilon_0 + \Delta t H_3 + (D\lambda^2\Delta t)^{1/2}(a_4\psi_1 + b_4\psi_2)) . \quad (4.12d)$$

V. TEST OF COLORED-NOISE PROPERTIES

To test how accurately these algorithms create colored noise, comparisons of the simulated correlations with the property

$$\{\langle \epsilon(t)\epsilon(t+s)\rangle\} = D\lambda \exp(-\lambda s) \quad (5.1)$$

are made. In these tests, the ϵ equation, (1.3b), has been integrated, leaving out the integration of an x equation. In order to give unbiased comparisons, all of the tests contain the same 100 initial ϵ values and use the same sequence of random numbers. The following figures show the results of the simulations for $\lambda = 1.0$ and for a range of a time differences up to $s = 4.0$. The integral algorithm is an exact method of simulating colored noise, so it is being used as a guide for how accurate the other algorithms are for a given set of random numbers. In Fig. 1, the time step used is rather large. But it shows the accuracy of both the integral algorithm, Fig. 1(a), and the SRKIV algorithm, Fig. 1(b). The SRKII algorithm, Fig. 1(c), is not as accurate for such a large time step, yet gives considerably better results than the Euler algorithm, Fig. 1(d). Figures 2(a)–2(d) show that for smaller time steps,

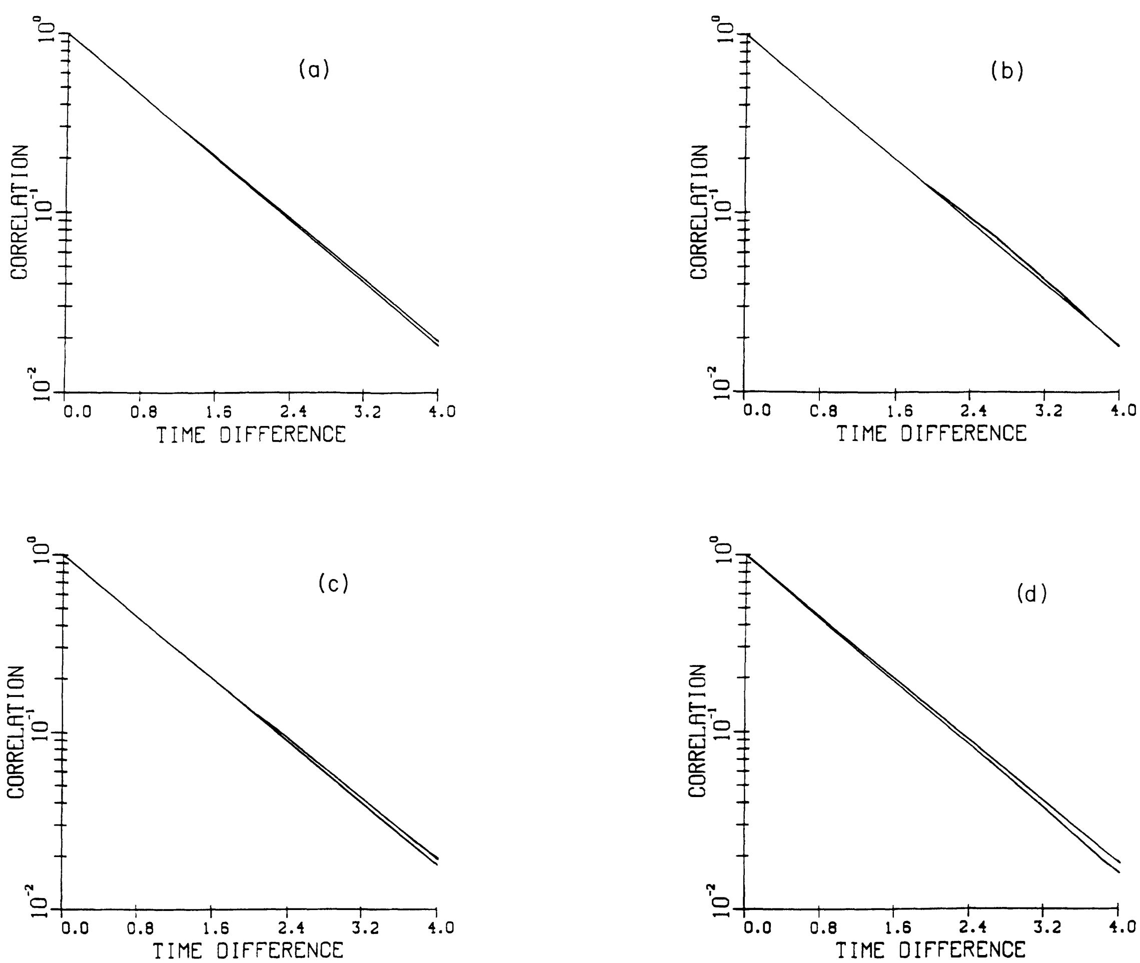

FIG. 2. The correlations are compared with a time step $\Delta t = 0.1$. Other values remain the same as Fig. 1. (a) Integral, (b) SRKIV, (c) SRKII, and (d) Euler.

the Euler algorithm still produces an incorrect slope, but the SRKII algorithm is indistinguishable from the integral algorithm. The difference in accuracy of the integral algorithm for the two time steps is a result of the random numbers. Although the SRKIV method is no less accurate than the integral and SRKII algorithms, it is distinguishable because it requires two sets of random numbers instead of one.

VI. MEAN FIRST-PASSAGE TIME IN A BISTABLE POTENTIAL

Next we consider motion in the bistable potential

$$U(x)=-\tfrac{1}{2}ax^2+\tfrac{1}{4}bx^4 \tag{6.1}$$

driven by exponentially colored noise. The dimensionless stochastic differential equation for this system is

$$\dot{x}=x-x^3+\epsilon(t)\ , \tag{6.2a}$$

$$\dot{\epsilon}=-\lambda\epsilon+\lambda g_w(t)\ , \tag{6.2b}$$

with

$$\{\langle\epsilon(t)\rangle\}=0\ , \tag{6.3a}$$

$$\{\langle\epsilon(t)\epsilon(t')\rangle\}=D\lambda\exp(-\lambda|t-t'|)\ . \tag{6.3b}$$

Consider the flow which is described by the deterministic portion of (6.2). This system has two stable fixed points at $\epsilon=0$, $x=\pm1$ and one unstable fixed point at $\epsilon=0$, $x=0$. The basins of attraction of the stable points are separated by the curve which passes through the unstable point. This separatrix curve is obtained by performing a time-reversed integration on the deterministic portions of (6.2).

The mean first-passage time [6,7] (MFPT) of a particle undergoing Brownian motion in this potential is the average time the particle takes to reach the separatrix starting from one of the valleys. Since the separatrix curve is obtained as a deterministic flow, it is most accurate for very small values of the noise strength D.

Unless otherwise specified, all values and graphs have been obtained using the value $D=0.1$, and an ensemble of 5000. In Fig. 3, the SRKII and the SRKIV methods are compared to the matrix-continued-fraction (MCF) method of Jung and co-workers for small $\tau=\lambda^{-1}$.

Since no exact solution can be found for the MFPT, many approximations have been developed for the different ranges of τ. Of the small τ theories [2,6],

$$T=\frac{\pi}{\sqrt{2}}\left[\frac{1+2\tau}{1-\tau}\right]^{1/2}\exp\left[\frac{1}{4D}\right]\ , \tag{6.4}$$

due to Hanggi, Marchesoni, and Grigolini, appears to be the most accurate. Figures 4(a) and 4(b) show our results compared with that of Eq. (6.4) after the normalization $T/T(0)$. The range of validity of this expression is from $\tau=0$ to approximately $\tau=0.6$.

For moderate τ values, the SRKII method was com-

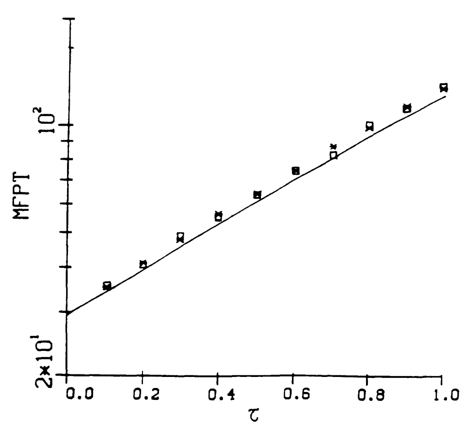

FIG. 3. Mean first-passage times for the bistable well. The squares are for the SRKII, asterisks for SRKIV, and the line corresponds to the matrix continued-fraction results of Jung and co-workers. An ensemble average of 5000 was used with $D=0.1$, and $\Delta t=0.1\tau$.

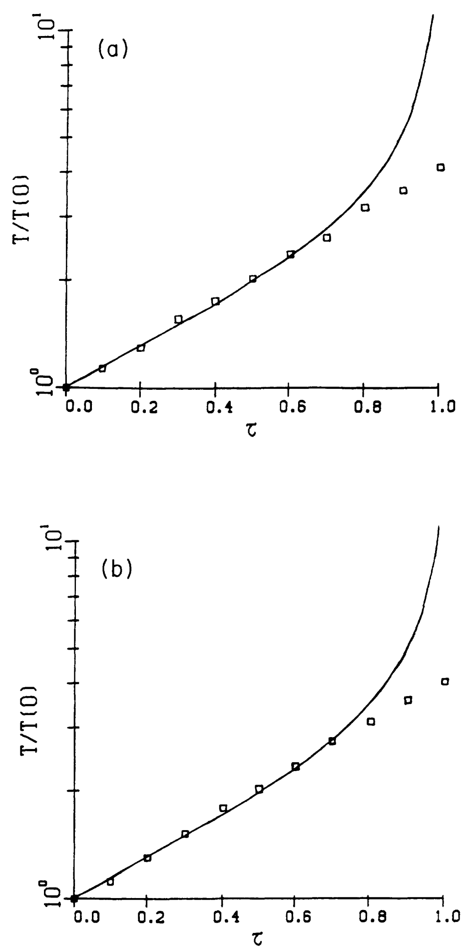

FIG. 4. Comparisons of simulated MFPT's to the small τ theory of Eq. (6.4). An ensemble average of 5000 was used with $D=0.1$, and $\Delta t=0.1\tau$. (a) SRKII and (b) SRKIV algorithms were used to obtain the squares.

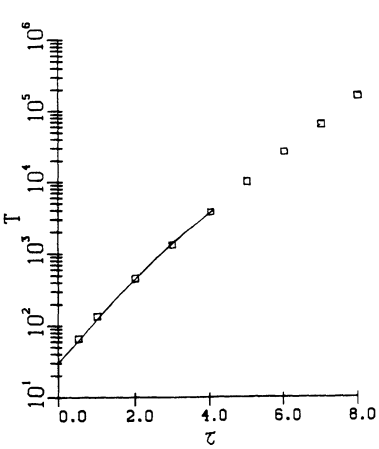

FIG. 5. MFPT comparison for intermediate τ. The solid line corresponds to matrix continued-fraction results of Jung and co-workers and the squares are the result of the SRKII algorithm. An ensemble average of 5000 was used with $D=0.1$, and $\Delta t=0.1\tau$.

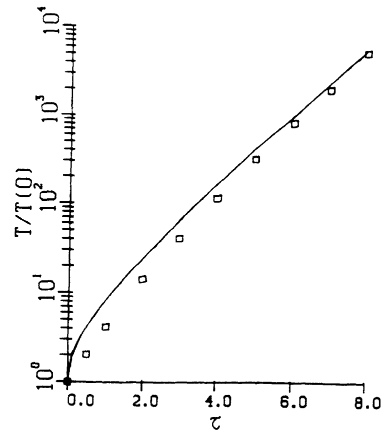

FIG. 6. MFPT comparison for large τ theory of Bray, McKane, and Newman with SRKII (squares). An ensemble average of 5000 was used with $D=0.1$, and $\Delta t=0.1\tau$.

pared to the MCF [8] calculations. This is shown in Fig. 5. The highest value we have from Jung, Hanggi, and Marchesoni [9] is for $\tau=4.0$.

For large τ, Bray, McKane, and Newman [10] obtained the expression

$$T=\text{const}\exp\left[\frac{\tau}{4D}\left[\frac{8}{27}+\lambda\tau^{-2/3}\right]\right], \tag{6.5}$$

with

$$\lambda=0.550\,844 .$$

This expression is plotted with our SRKII data in Fig. 6. The expression does not agree exactly for our largest τ, but for slightly larger τ there is good potential for agreement. Testing the validity of (4.18) for these larger τ values requires an extremely large amount of computer time.

VII. CONCLUSIONS

In conclusion, it has been shown that these algorithms create more accurate correlation properties, and they generate accurate MFPT values. Only the time-independent case has been considered in this paper, but the same procedure of development should lead to time-dependent algorithms as well. It would also be expected that multiplicative noise could be dealt with in the same manner. And finally, the same procedure could be used for multivariable equations, most likely resulting in a larger number of random variables.

ACKNOWLEDGMENTS

I would like to thank the Physics Department at Georgia Institute of Technology, where this work was done, and Ronald Fox for the many discussions over the past few years.

[1] F. Fox. I. R. Gatland, R. Roy, and G. Vemuri, Phys. Rev. A **38**, 5938 (1988).
[2] P. Hanggi, F. Marchesoni, and P. Grigolini, Z. Phys. B **56**, 33 (1984).
[3] S. Zhu, A. W. Yu, and R. Roy, Phys. Rev. A **34**, 4333 (1986).
[4] W. H. Press, B. P. Flannery, S. A. Teukolsky, and W. T. Vetterling, *Numerical Recipes: The Art of Scientific Computing* (Cambridge University Press, New York, 1986).
[5] R. L. Honeycutt, Ph.D. dissertation, Georgia Institute of Technology, 1990.
[6] R. F. Fox, Phys. Rev. A **37**, 911 (1988).
[7] P. Hanggi, P. Jung. and F. Marchesoni, J. Stat. Phys. **54**, 1367 (1989).
[8] P. Jung and H. Risken, Z. Phys. B **61**, 367 (1985).
[9] P. Jung, P. Hanggi, and F. Marchesoni, Phys. Rev. A **40**, 5447 (1989).
[10] A. J. Bray, A. J. McKane, and T. J. Newman, Phys. Rev. A **41**, 657 (1990).